

An Approach to the Electroanalysis of Electrode Passivating Analytes: The Determination of Phenol

Yuanzhe Wang and Richard G Compton^{*,[a]}

The electrode-passivating species, phenol, was electrochemically determined by using semicircular sweep voltammetry on a basal-plane pyrolytic graphite (BPPG) electrode. The electrode fouling caused by the polymerization of phenol was prevented at low concentrations by introducing a second species, 4-

amino-2,6-dichlorophenol (PAP), to prevent the polymerization of phenol in the vicinity of the electrode surface. Semicircular sweep voltammetry was used to amplify the analytical signal, realizing the detection of phenol in the concentration range of 25–800 μM without problems of electrode fouling.

1. Introduction

The many attractions of amperometric electro-analysis – sensitivity, low cost, ease of use and sometimes selectivity – are well rehearsed and in favorable situations conventional voltammetry,^[1] often enhanced by pulse voltammetry^[2] where necessary, can allow the practical measurement of many and diverse analytes ranging from gas sensors for oxygen,^[3] hydrogen sulfide,^[4] anesthetic gases^[5] of carbon monoxide in smoke detectors, to enzyme electrodes most notably for blood glucose,^[6] to bacteria^[7] and to specialist pH measurements^[8] as is evident from the ever increasing variety of such electrochemical sensors sold commercially.^[9]

The generic feature of amperometric sensors, namely the generation of a concentration related Faradaic current, requires sustained oxidation or reduction of the analyte of interest, at least for a sufficient time for a meaningful measurement to be made. Whilst this is clearly possible in the many cases alluded to above given the correct choices of electrode materials, electrode geometries, solvents, and in aqueous systems pH, as well as the potentials applied to the electrode, in other cases the electrolysis induces the passivation of the electrode surface precluding useful analytical measurement. An example of this occurs in the electro-oxidation of phenols where the generated phenoxy radical polymerize onto the electrode surface leading to the rapid passivation of the electrode.^[10]

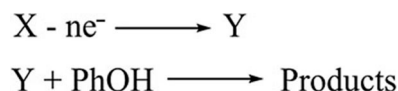


The passivation is sufficiently strong and rapid to prevent the electro-analysis of concentrations of phenol above a critical

threshold above, which meaningful analysis is impossible on the timescale of the sought voltammetric measurement.

To overcome the electrode fouling problem with phenol, various electrode materials and modifications were suggested in the literature.^[11] However, the electrode modifications require elaborate and complicated procedures and produce surfaces which often have only a short lifetime sometimes being limited to a single analytical measurement. Use of an unmodified electrode is much more convenient and often gives more repeatable results comparing to using a modified electrode.

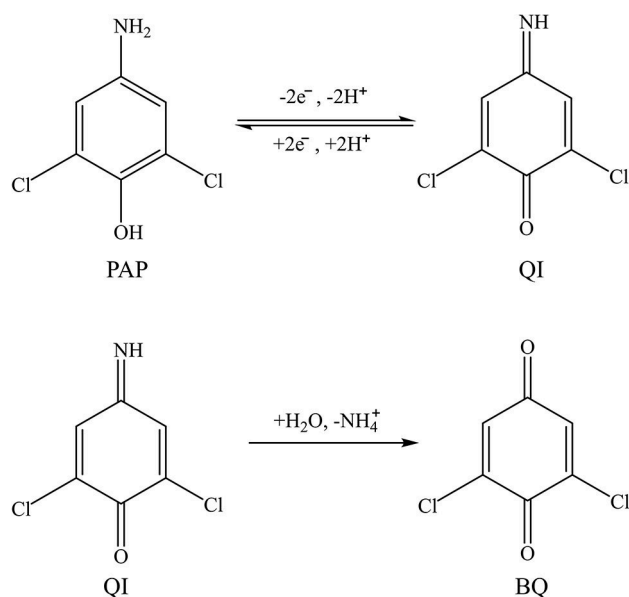
In the present paper we develop a likely generic approach to the solution of the electrode passivation problem in the specific context of phenol oxidation at an unmodified carbon electrode in which a second species (Y) is generated electrochemically from an introduced additive, X, and used to diminish the concentration of phenol undergoing direct oxidation at the electrode by virtue of the reaction:



where the products are soluble. In the approach taken this process occurs in parallel with the oxidation of phenol to the extent that the magnitude of the phenol concentration is the vicinity of the electrode is reduced below the threshold value required for polymerization and hence for electrode passivation. In the following we use the two electron oxidation of 4-Amino-2,6-dichlorophenol (PAP) acting as species X to generate the quinonimine species Y as shown in Scheme 1,^[12] noting that the quinonimine undergoes slow hydrolysis on the voltammetric timescale as also shown in Scheme 1. The oxidation of PAP occurs at less positive potentials than those required for the oxidation of phenol. Thus, if a voltammetric scan is made two features are apparent; first the oxidation of PAP to Y at low positive potentials and second the analytically useful oxidation of phenol at more positive values. Of course, the 'dilution' of the phenol concentration in the vicinity of the electrode leads to a decrease in the analytical signal in comparison to what might be observed if, hypothetically, the phenol could be directly oxidized without electrode passivation. Hence in order

[a] Y. Wang, Prof. Dr. R. G Compton
Department of Chemistry, Physical and Theoretical Chemistry Laboratory,
Oxford University, South Parks Road, Oxford OX1 3QZ, UK
E-mail: yuanzhe.wang@wadham.ox.ac.uk
richard.compton@chem.ox.ac.uk

© 2020 The Authors. Published by Wiley-VCH GmbH. This is an open access article under the terms of the Creative Commons Attribution License, which permits use, distribution and reproduction in any medium, provided the original work is properly cited.



Scheme 1. Structures of PAP (X) and its oxidised products quinoneimine (QI) and benzoquinone (BQ).

to boost the sensitivity in the experiments reported below, we replace the conventional linear sweep voltammetry (LSV) by the recently advocated 'semicircular' voltammetry^[13] so as to apply a voltage scan rate which is relatively slow at the potentials required for PAP oxidation but significantly faster in the region of the phenol oxidation (Figure 1). As depicted in Figure 1, the terms 'slow' and 'fast' are relative to the average scan rate throughout the semicircular scan. This has the effect of, first, generating a relatively thicker reaction layer of Y near the electrode for homogeneous chemical reaction with phenol as a result of the initially slower scan. Second, it has effect of enhancing the size of the peak current for the phenol oxidation and hence also the analytical signal because of the transiently faster scan rate at the potential of analysis. In this way higher

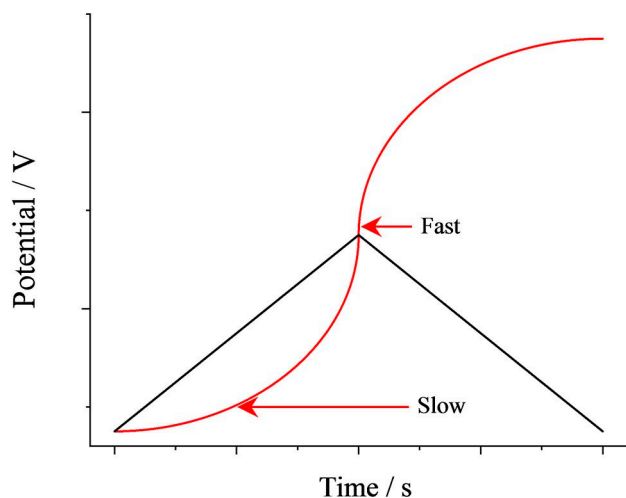


Figure 1. Waveforms of cyclic voltammetry (black line) and semicircular sweep voltammetry (red line) at the same average scan rate.

concentrations of phenol of up to ca. 800 micro-molar can be analyzed quantitatively.

2. Results and Discussion

In the following sections, first, the voltammetric response of phenol in a pH 10 borate buffer solution at a BPPG electrode is examined and the electrode fouling problem was identified. Next, the electrochemical behavior of PAP is reported followed by that of phenol in the presence of PAP and a possible mechanism is inferred with respect to the crucial role of PAP in protecting the electrode surface which facilitates phenol electro-analysis. Finally, in the system with PAP present, semi-circular sweep voltammetry is employed to realize a sensitive electroanalytical detection of phenol under an optimized potential window. The method was optimized.

2.1. Electrochemistry of Phenol

We first examined the initial voltammetric response of phenol in a pH 10 borate buffer solution at a BPPG electrode. Figure 2 depicts the cyclic voltammograms of 1 mM phenol in the pH 10 borate buffer solution recorded at a scan rate of 50 mVs⁻¹. An electrochemical oxidation peak is seen at ca. +0.50 V vs. SCE and was found to decrease significantly over multiple scans. The apparent oxidative transfer coefficient (β)^[15] was determined to be 0.85 using Tafel analysis of the first scan (Figure 3), which suggests the near reversible behavior was observed for phenol at the applied scan rate. Hence, the total number of electrons transferred corresponding to phenol oxidation was estimated in two different ways using a diffusion coefficient in aqueous solution, reported as 9.2 × 10⁻¹⁰ m²s⁻¹ at 295 K in literature,^[16] namely *via* both the irreversible and reversible, multiple electron-transfer *Randles-Sevcik* equations^[1] as 2.3 and

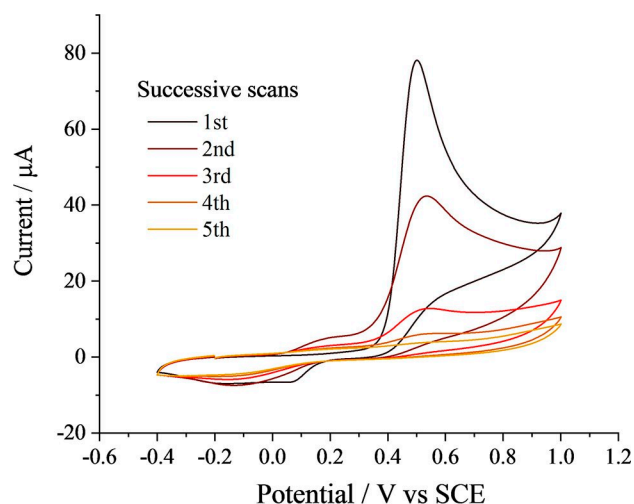


Figure 2. Cyclic voltammograms of successive scans of 1 mM phenol in a pH 10 borate buffer solution at a BPPG electrode. The scan rate was 50 mVs⁻¹.

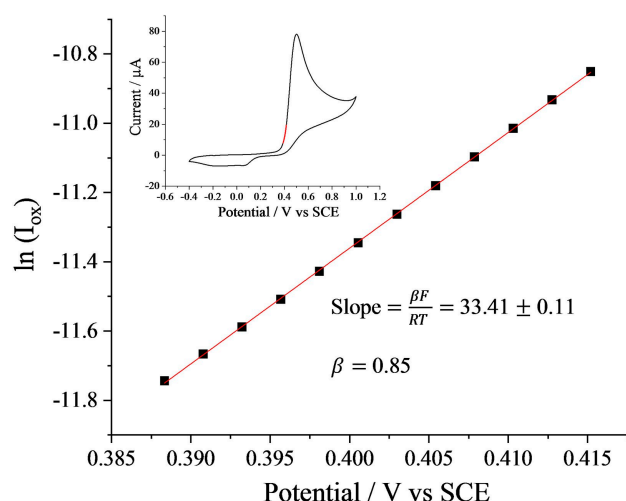


Figure 3. Tafel analysis for voltammogram of 1st scan of 1 mM phenol electro-oxidation. The scan rate was 50 mV s⁻¹. Inset shows the 1st scan voltammogram (black line) and the Tafel analysis region (highlighted in red region), where diffusion has almost negligible effect on.

2.2, respectively. The above features can be interpreted as a multi-step process, including the de-protonation, oxidation, and polymerization of phenol^[10,17] (Scheme 2). At the pH values near or higher than the pK_a of phenol (9.98, 25 °C),^[18] phenol is deprotonated and oxidized to phenoxy radical in the first step, with fast (near reversible) electrode-kinetics^[1] in a one-electron-transfer process, as indicated by the large β value close to 1. The phenoxy radical is then thought to react with other phenoxy radicals and/or phenol and undergo polymerization, which is responsible for the observed large total number of electrons transferred. It has been reported that the polymeric and oligomeric products formed strongly adsorbed, insulating layers on the electrode surface.^[10,17] As shown in Figure 2, the layers clearly have a pronounced, accumulating effect on the analytical responses of phenol oxidation on the BPPG electrode over a short time period, diminishing the signal rapidly from over 80 μ A to near 0 μ A and precluding direct analysis.

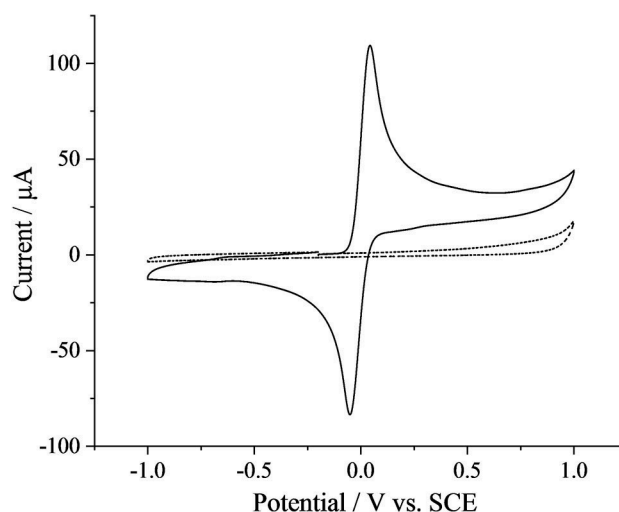
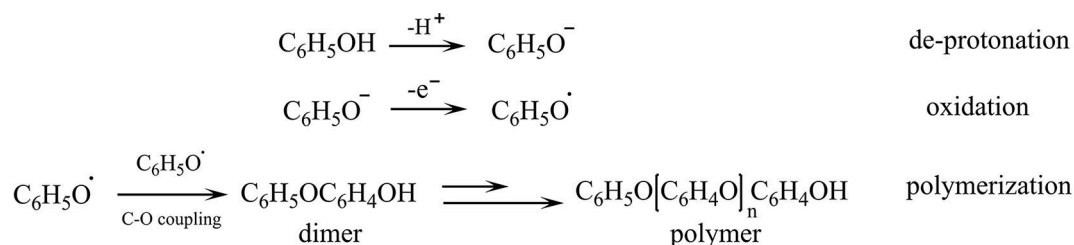


Figure 4. Cyclic voltammetric responses of 1 mM PAP (solid line) and background (dash line) in the pH 10 borate buffer solution at the BPPG electrode. The scan rate was 100 mV s⁻¹.

2.2. Phenol Detection in the Presence of PAP

2.2.1. Electrochemistry of PAP

The electrochemical behavior of PAP in pH 10 borate buffer solution on BPPG was studied first and the results compared with previous studies.^[11,18] The cyclic voltammetric response of 1 mM PAP recorded at 100 mV s⁻¹ in Figure 4 shows an oxidation peak at ca. +0.04 V vs SCE and a corresponding backward reduction peak at ca. -0.05 V vs SCE. The effect of variable scan rates on the oxidation peak currents of PAP was studied in the range of 5–400 mV s⁻¹. Figure 5 shows the cyclic voltammograms recorded at the varying scan rates in the studied range. The peak heights were found to exhibit a linear dependence of the square root of scan rate, indicating a diffusion-controlled process (Inset of Figure 5). Tafel analysis was performed on several cyclic voltammograms, revealing the transfer coefficient value (β) of ca 1.5. It can be confirmed from the β values that the oxidation of PAP corresponds to a two-electron transfer process, where the second electron transfer is rate determining step.^[1] Using a β value of 1.5 obtained from the voltammograms recorded at a moderate scan rate of 25 mV s⁻¹ (Figure 6), the diffusion coefficient at 295 K for a two electron-transfer process can be estimated to be 4.5 ×



Scheme 2. Electro-polymerisation of phenol at the BPPG electrode in the pH 10 borate buffer solution.

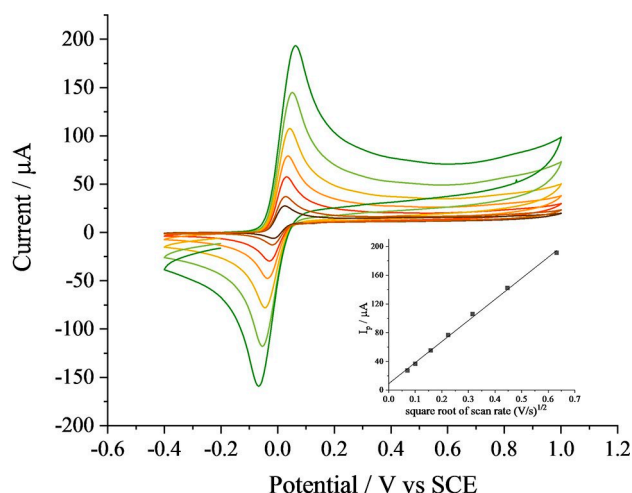


Figure 5. Cyclic voltammograms of 1 mM PAP in the pH 10 borate buffer solution at the BPPG electrode recorded at scan rates of 5 mVs⁻¹, 10 mVs⁻¹, 25 mVs⁻¹, 50 mVs⁻¹, 100 mVs⁻¹, 200 mVs⁻¹, 400 mVs⁻¹. Inset: plot of peak current (background corrected) versus square root of scan rate.

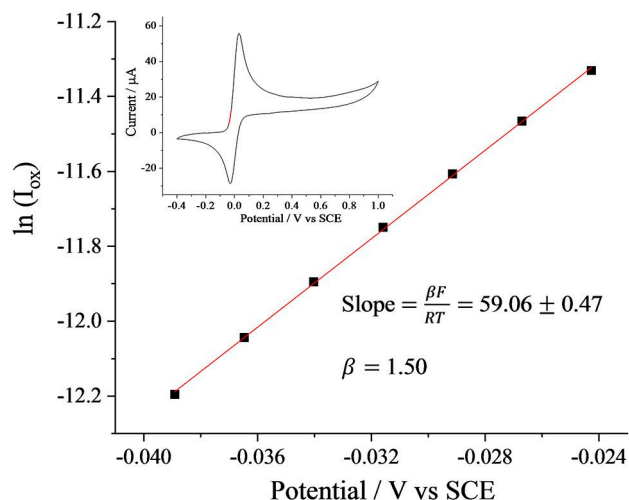


Figure 6. Tafel analysis for voltammogram of 1 mM PAP recorded at the scan rate of 25 mVs⁻¹. Inset shows the voltammogram recorded at 25 mVs⁻¹ (black line) and the selected Tafel analysis region (highlighted in red region) where the diffusion effect is almost negligible.

10⁻⁶ cm²s⁻¹, in agreement with the diffusion coefficient values of PAP reported in literature.^[19,20]

It can be seen in Figure 4 and Figure 5 that the reduction peaks are smaller than the corresponding oxidation peak, suggesting a loss of the oxidized product from a possible further reaction. The instability the oxidized product generated in the forward scan can be identified by comparing the ratios of oxidation peak currents to reduction peak currents at the varying scan rates in the range of 5–400 mVs⁻¹ (Table 1). With the increase of scan rate, the loss of reduction peak on the reverse scan becomes less significant since less time is given to the oxidized product for the next-step reaction during the voltammetric measurement.^[1] The observed features are consistent with the literature, where the reactions have been reported as a two electron, two proton transfer processes

Table 1. Ratios of the oxidation peak currents to the reduction peak currents (both background-corrected) at varying scan rates from 5 to 400 mVs⁻¹.

Scan rate [mVs ⁻¹]	5	10	25	50	100	200	400
<i>I</i> _p ox/ <i>I</i> _p red ratios	1.66	1.59	1.43	1.32	1.20	1.09	1.08

occurring between PAP-QI redox couple, followed by a slow hydrolysis step of QI to form BQ via an EC mechanism (Scheme 1).^[12,19] In the above the PAP electro-oxidation mechanism and the electron transfer steps have been examined and the diffusion of PAP characterized. We next turn to the oxidation of PAP is the presence of phenol.

2.2.2. Phenol Detection in the Presence of PAP using CV

We next explored the role PAP playing in the electrochemical process of phenol oxidation and the possible electroanalytical detection of phenol in the presence of PAP using CV. Phenol was added to a pH 10 borate buffer solution containing 1 mM PAP to give concentrations in the range of 25–800 μM. The cyclic voltammetric responses of the solutions with additions of 0–800 μM phenol on the BPPG electrode were recorded at 50 mVs⁻¹ and shown in Figure 7 (A). Two major changes of voltammograms with the increasing concentrations of phenol additions can be observed. First, for the peaks expected for the PAP-QI redox reactions, a noticeable decrease was seen for the reduction peaks at ca. -0.04 V vs. SCE with increasing concentrations of phenol from 25 μM to the maximum concentration of 800 μM, where the peak height was reduced to near zero. The change in the oxidation peaks at +0.04 V vs. SCE were negligible. Previous studies suggest^[21] under conditions of pH=9–10, phenol or some substituted phenols can react with dichloro-benzoquinone monoamine, in what is known known as the 'Gibbs reaction'. The latter is often used in *homogeneous* solution for phenol detection via chemical oxidation of a dichloro-aminophenol, such as PAP. In Figure 7 (A) the decreasing backward reduction peak heights can be inferred as a result of losing oxidized PAP owing to the Gibbs reaction with increasing amounts of phenol, and possibly, further reaction with phenoxy radicals. The second feature shown to change with the additions of phenol is that a new peak at ca. +0.51 V vs. SCE has emerged and grown with the increasing phenol concentration. This is most likely due to the direct oxidation of phenol, which switches on at a very similar potential of +0.50 V vs. SCE to that seen in Figure 2 for the oxidation of phenol in the absence of PAP. The second peak will be further investigated using semicircular voltammetric signals below. Prior to that the interaction of phenol with oxidized PAP was clarified.

Figure 7 (B) depicts the cyclic voltammogram swept from the same starting potential of -0.2 V vs. SCE but reversed at 0.3 V vs. SCE, before the onset of the second oxidation, leaving only the unreacted phenol with the oxidized PAP in the reaction system. A similar trend of a decrease in the peak height of reduction peak with the increase of phenol concentration can

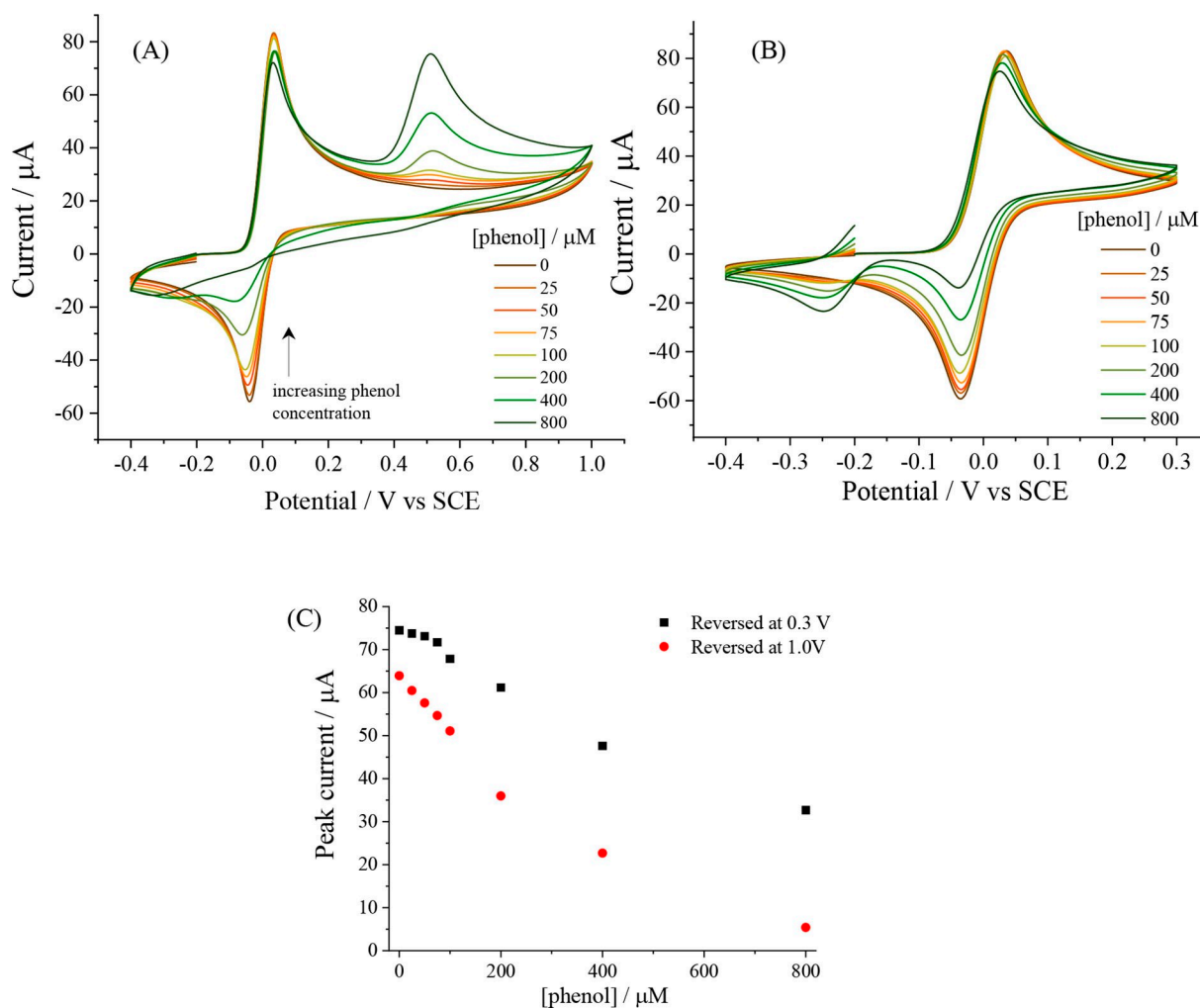


Figure 7. Cyclic voltammetric responses of phenol addition to the pH 10 borate buffer solution containing 1 mM PAP, swept from -0.2 V to $+1.0$ V (A), and $+0.3$ V (B) vs. SCE. The scan rate was 50 mVs $^{-1}$. C) Comparison of the reduction peaks currents (background-corrected) obtained from (A) and (B).

be seen in Figure 7 (B) as compared to Figure 7 (A) but with a significantly less sensitivity to the amount of phenol present as seen in Figure 7 (C). It can be inferred that phenol and the product of the second oxidation, which much likely to be phenol radicals from the direct oxidation of phenol are both involved in the reaction with the oxidized PAP. In Figure 7 (B), additional reduction peaks were observed for the higher phenol concentrations as a result of the greater participation of phenol in the reaction with oxidized PAP without the presence of phenol radicals.

In order to investigate the mechanism in the light of the known Gibbs reaction and, in particular, to understand the participation of phenol and the electro-oxidized phenol in the reaction with oxidized PAP, successive cyclic voltammetric measurements were conducted for varying concentrations of phenol. The effect of PAP on the electrode fouling caused by phenol, as discussed in Section 2.1 was investigated. As can be seen in Figure 8, in the phenol concentration range of 25–100 μM, the PAP oxidation peaks showing ca. 30% decrease in peak currents over five cycles regardless of the presence of phenol. However, the peak currents of the second oxidation

peak corresponding to the direct oxidation of phenol remained unchanged over five scans. It can be inferred the electrode surface was protected from the formation of the previously discussed polymeric film, which results from the oxidation of phenol and precludes useful analysis of high phenol concentrations. Combining the above observations, a possible mechanism where PAP acting as a mediator preventing the electrode passivation during phenol electro-oxidation can be suggested (Scheme 3). Firstly, phenol was deprotonated and the oxidation occurred. Next, QI generated from oxidation of PAP becomes involved and reduces the amount of phenol in the locality of the electrode via either direct reaction with phenol and oxidized phenol, avoiding the products may 'block' the electrode, including problematic polymers at the remote reaction layer. In other words, the oxidized PAP allows the possible electro-analysis of phenol at the corresponding potential by preventing electrode fouling by reducing the critical threshold concentration of oxidized phenol needed to form the blocking polymeric layer. It is possibly achieved by also shifting some of the overall phenol oxidation reaction physically away from electrode surface into an adjacent reaction

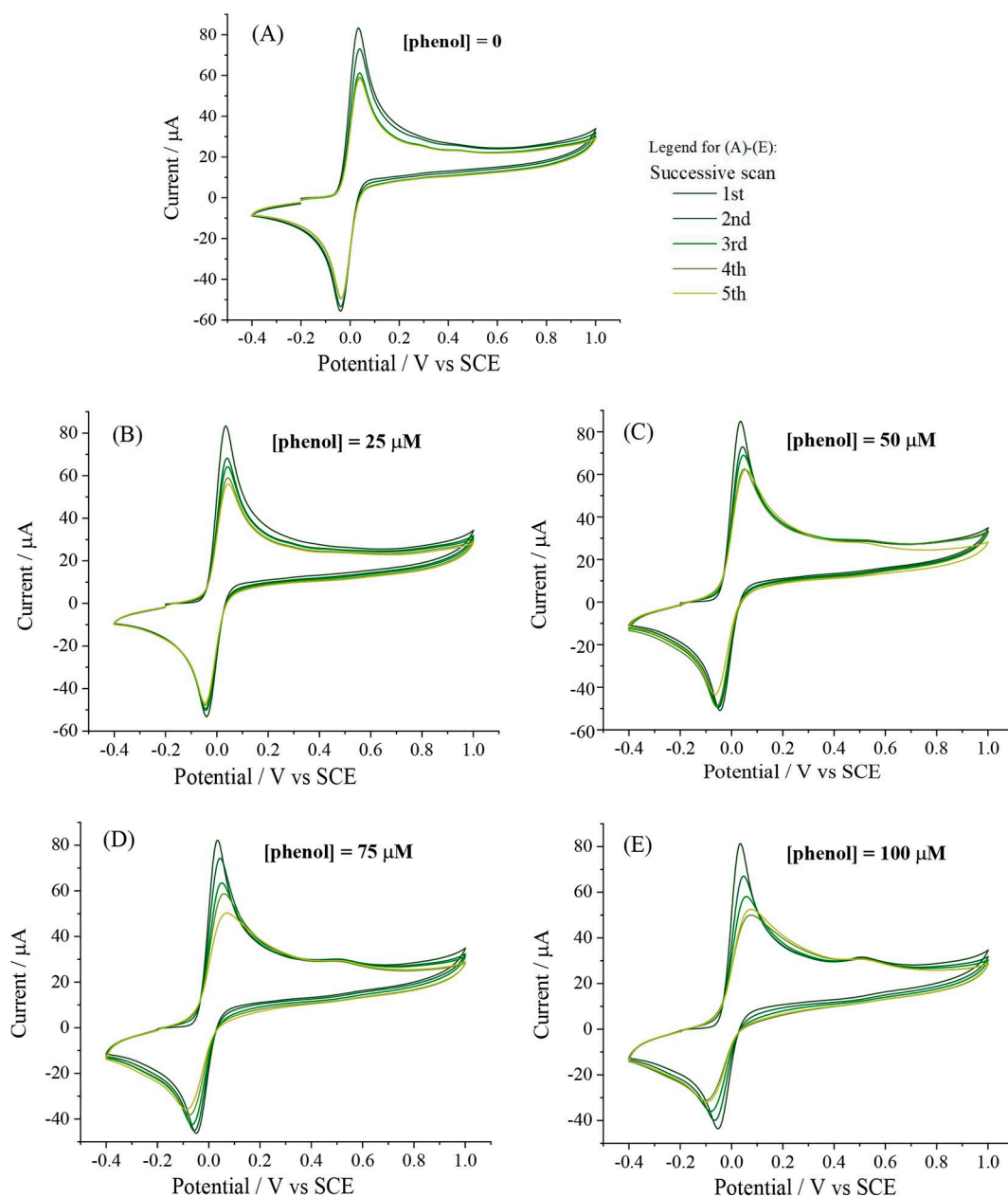
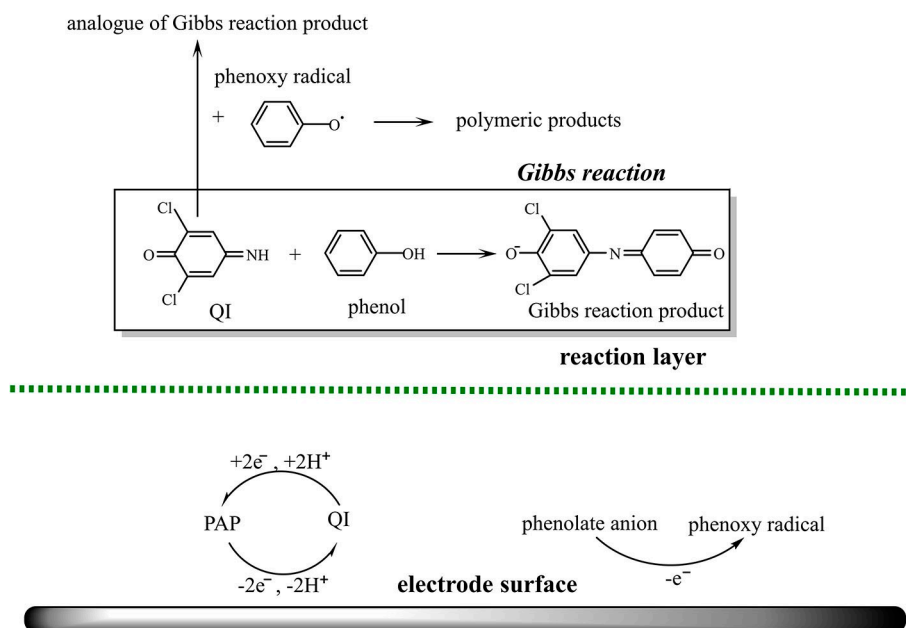


Figure 8. Cyclic voltammetric responses of A) 0, B) 25 μM , C) 50 μM , D) 75 μM , E) 100 μM phenol addition to 1 mM PAP in the pH 10 borate buffer solution at the BPPG electrode recorded for multiple scans at a scan rate of 50 mVs^{-1} .

layer. This provides a basis for establishing the method of phenol quantification by adding 1 mM PAP in the pH 10 system to detect phenol in the concentration range of 25–100 μM , where a protected, clean electrode surface at the required potential for phenol oxidation is ensured. However, although, as shown by the stability of the phenol oxidation peak in Figure 8, the approach allows for reproducible oxidative voltammetry of phenol it necessarily reduces the size of the phenol oxidation peak over what, hypothetically, would be seen if the direct oxidation could proceed without electrode fouling. In the following section we suggest how this drawback can be overcome and remedied.

2.2.3. Phenol Detection in the Presence of PAP using Semicircular Sweep Voltammetry

Having investigated the electrochemical process of phenol with the presence of PAP in the studied system, we now turn to developing the method to enhance the electroanalytical performance of phenol using semicircular sweep voltammetry. As discussed in previous studies,^[12,22] applying a semicircular potential wave over a chosen potential window can selectively amplify the current responses in the vicinity of the midpoint of the potential window (defined as E_{mid}), where scan rate reaches a near infinite value (reflecting, experimentally, ultimately the limitations of the potentiostat employed). The approach



Scheme 3. Mechanism of phenol oxidation in the presence of PAP and 'electrode protection' in the pH 10 borate buffer solution at the BPPG electrode.

correspondingly suppresses the current responses at the other regions, where the scan rate is relatively slow. The semicircular sweep voltammetric responses of 100 μM phenol with the presence of 1 mM PAP in the pH 10 borate buffer solution at the BPPG electrode were recorded at varying potential windows. The potential window was adjusted by shifting E_{mid} from -0.15 to $+0.75$ V vs. SCE whilst held at the same scan amplitude of 0.8 V and the same average scan rate of 50 mVs^{-1} . Three peaks can be seen in Figure 9 changing with the potential windows. Two of them are the oxidation peaks (seen at ca. $+0.04$ V and ca. $+0.50$ V vs. SCE respectively for a potential window with E_{mid} of $+0.375$ V) due to the PAP and phenol oxidation reactions. The third sharp peak (at $+0.375$ V

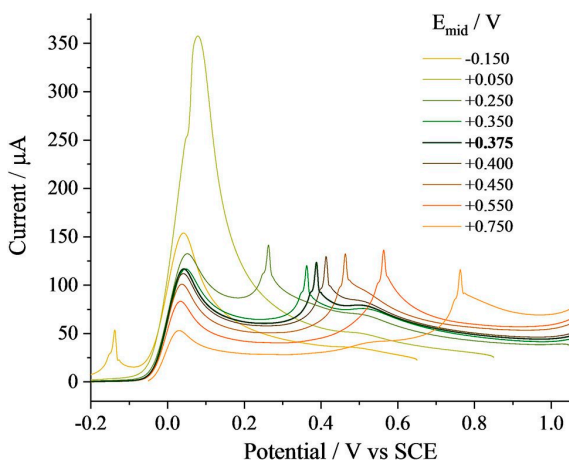


Figure 9. Semicircular sweep voltammetric responses of 100 μM phenol in the pH 10 borate buffer solution containing 1 mM PAP at the BPPG electrode recorded at potential windows with varying E_{mid} . The average of scan rate was 50 mVs^{-1} . The scan amplitude was 0.8 V.

vs. SCE, the midpoint of the potential window) arises from the transiently nominally infinite scan rate (within limitations of the potentiostat electronics), which, as previously noted^[12,21] is attributed to strong capacitive charging currents. With the adjustment of potential windows, the two oxidation peak currents increased significantly when E_{mid} approached to their oxidation potentials and decreased when E_{mid} moved away from the oxidation potentials. The sharp peak was shown to affect the sizes and shapes of two oxidation peak as E_{mid} was close to the oxidation potentials of two peaks and even merged with the bigger PAP peak when E_{mid} moved to $+0.05$ V vs SCE. Thus, as suggested by Figure 9, with a fixed scan amplitude of 0.8 V, the E_{mid} of potential window was optimized as $+0.375$ V vs SCE to give the largest possible size as well as a clearly distinguishable shape of the phenol related peak.

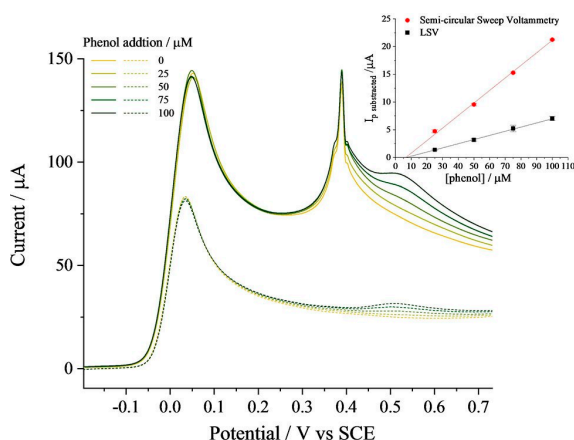
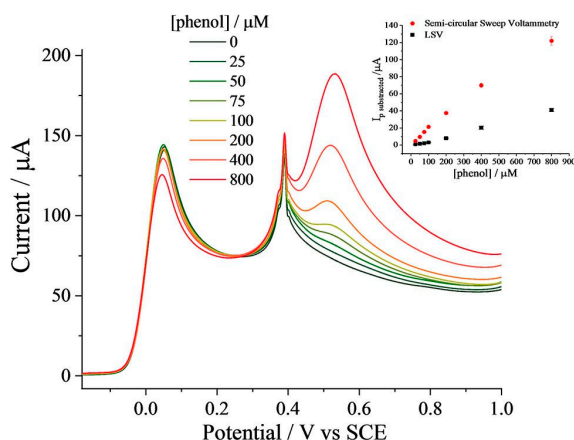
Three repeating sets of phenol solutions within the chosen concentration range of 0–100 μM (Section 2.2.2) were prepared and the signals of each solution were measured in the developed system present with 1 mM PAP using semicircular sweep voltammetry. All peak currents were obtained by subtracting the zero concentration current values, which was read at a fix potential near the peak potential in the voltammogram in absence of phenol, from the current values read at the same, fixed potential in the voltammograms of 25–100 μM phenol. The peak currents were plotted against phenol concentrations for the evaluation of detection sensitivities. Table 2 recorded the slopes values peak current-concentration plots at a range of scan amplitudes from 0.2 V to a maximum of 1.0 V, constrained by the need for the phenol oxidation peak to remain distinguishable from the sharp peak at E_{mid} , which grew with the increasing scan amplitudes. As suggested in Table 2, the potential window with a large scan amplitude of 1.0 V and the E_{mid} of $+0.375$ vs SCE leads to the largest slope values, thus

Table 2. Slope values of the plots of phenol peak currents against phenol concentration obtained from the voltammograms of 0–100 μM of phenol in the pH 10 borate buffer solution present with 1 mM PAP recorded at varying scan amplitudes. The average scan rate was 50 mVs^{-1} .

	LSV	Semicircular sweep voltammetry					
Scan amplitude [V]		0.20	0.30	0.35	0.425	0.80	0.90
E_{mid} [V vs SCE]		0.375	0.325	0.350	0.325	0.375	0.375
Slope of I_p [μA] vs. [phenol] [μM] plot	0.072	0.10	0.10	0.11	0.14	0.20	0.21

can be used as an optimal for a fast and sensitive detection of phenol.

In Figure 10, the semicircular sweep voltammetric responses recorded using the potential window thus optimized are compared with the linear sweep voltammetric responses of the studied concentration range of phenol in the system present with PAP recorded at the same average scan rate (50 mVs^{-1}). It is evident the phenol oxidation peak was largely amplified when the semicircular potential sweep was applied. The peak

**Figure 10.** Semicircular sweep (solid lines) vs linear sweep (dash lines) voltammetric responses of 0–100 μM phenol in the pH 10 borate buffer solution containing 1 mM PAP recorded at the potential windows with E_{mid} of +0.375 V vs. SCE and scan amplitude of 1.0 V.**Figure 11.** Semicircular sweep voltammetric responses of 0–800 μM phenol in the pH 10 borate buffer solution containing 1 mM PAP recorded at the optimized potential window. The average of scan rate was 50 mVs^{-1} . Inset: Plot of subtracted peak currents obtained from linear and semicircular voltammograms versus phenol concentration.

currents analyzed from semicircular sweep voltammogram show a linear dependence on phenol concentration in the range of 25–100 μM , which can be described as: $I_p/\mu\text{A} = (0.22 \pm 6.9 \times 10^{-3}) [\text{phenol}] (\mu\text{M}) + (1.49 \pm 0.59) (\mu\text{A})$, $N=4$, $R^2=0.998$ (Inset of Figure 10). The sensitivity of detection was improved ca. 3 times comparing to employing the conventional LSV (table 2). In both cases, strong dependences on the phenol concentration were found for the second oxidation peak current, revealing marked contributions from the direct oxidation of phenol. This has now been demonstrated from the analytical perspective.

Next semicircular sweep voltammetry of higher concentrations of 200–800 μM of phenol in the presence of 1 mM PAP was performed using the optimized potential window. Figure 11 records the semicircular voltammograms of phenol in the range of 0–800 μM and the inset graph compares the peak currents obtained from semicircular and linear voltammograms graph. It can be seen that the greatly amplified current responses of the second peak offer the better sensitivity of signals to phenol concentrations over the whole concentration range, suggesting the advantage of semicircular sweep voltammetry to linear sweep voltammetry in the electro-analysis of interest due to its selective amplification facilitated by the adjustment of potential windows and high sensitivity.

Finally, we looked into the possibility of further improving the sensitivity by raising the average scan rate to 200 mVs^{-1} . Table 3 summarizes the detection sensitivity of phenol in the concentration range of 25–100 μM in the presence of 1 mM PAP using LSV and semicircular sweep voltammetry. It is evident that over a fixed potential window, applying higher average scan rates facilitates a more sensitive phenol detection over the studied concentration range, although semicircular sweep voltammetry offers a relatively greater advantage over the conventional LSV at the lower average scan rate.

Table 3. Slope values of the plots of phenol peak currents against phenol concentration which obtained from the voltammograms of 0–100 μM of phenol in the pH 10 borate buffer solution present with 1 mM PAP recorded at varying scan rates using LSV and semicircular voltammetry.

	Slopes of I_p [μA] vs. [phenol] [μM] plots at varying scan rates [mVs^{-1}]			
	25	50	100	200
LSV	0.053	0.072	0.13	0.17
Semicircular sweep voltammetry	0.19	0.22	0.31	0.36

3. Conclusions

We developed an electroanalytical method for the detection of high concentrations of phenol without the problem of electrode fouling by introducing a second species, PAP, into the solution to be studied, facilitating phenol detection via a possible 'electrode protection' mechanism. Semicircular potential sweep voltammetry was applied to amplify the analytical signal. Under an optimized potential window with the scan amplitude of 1.0 V centered on a potential of +0.375 vs SCE, phenol concentrations in the range 25–800 μM were measured without problems of electrode fouling.

Experimental Sections

Chemicals and Reagents

All chemicals were of analytical grade and were used received without any further purification. PAP (97%) was purchased from Alfa Aesar and phenol (99.0–100.5%) was purchased from Sigma-Aldrich. All aqueous solutions were prepared with deionized water at a resistivity of 18.2 $\text{M}\Omega\text{ cm}$ at 298 K (Millipore, MA, USA). The borate buffer solution (0.1 M) was used as supporting electrolyte and was prepared using sodium tetraborate (Sigma-Aldrich, 97%) and sodium hydroxide (Sigma-Aldrich, 97%). The borate buffer solution was made at pH = 10.0 and checked with a Hach Lange Sension + PH31 pH meter. Stock solutions of phenol (10 mM) was prepared by dissolving phenol in ethanol (Sigma-Aldrich, $\geq 99.8\%$). Stocked solution was then diluted with aqueous solutions to required concentrations.

Apparatus

All electrochemical experiments were performed in a Faraday cage at 295 K using a three-electrode configuration. Cyclic voltammetric measurements were carried out using a $\mu\text{Autolab II}$ potentiostat (Metrohm-Autolab BV, Netherlands). Semicircular sweep voltammetric measurements were performed using an in-lab built potentiostat giving low-noise measurements and a high sampling rate of 100 kHz.^[14] The in-lab built potentiostat was controlled by software Python 3.5 to generate required potential waveforms. For all experiments, a basal plane pyrolytic graphite (BPPG) with a 4.9 mm diameter was used as the working electrode, a saturated calomel electrode (SCE, ALS distributed by BASi Inc., Japan.) was used as the reference electrode and a platinum wire was used as the counter electrode. The working electrode was polished using soft lapping pads with alumina of decreasing particle sizes (1.0, 0.3 and 0.05 μm) (Buehler, IL, UK), followed by sonication in water. Solutions were bubbled with nitrogen for 10 minutes before each measurement.

Conflict of Interest

The authors declare no conflict of interest.

Keywords: electroanalysis • phenol • polymerization • sensors • semicircular sweep voltammetry

- [1] a) J. Wang, *Analytical electrochemistry*, 3rd ed., Wiley-VCH, Hoboken, N. J., 2006; b) R. G. Compton, C. E. Banks, *Understanding voltammetry*, 3rd ed., World Scientific Publishing Europe, London, 2018.
- [2] Á. Molina, J. González, in *Monographs in electrochemistry*, Springer, Cham, 2016.
- [3] L. C. Clark, R. Wolf, D. Granger, Z. Taylor, *J. Appl. Physiol.* **1953**, 6, 189–193.
- [4] P. Jeroschewski, K. Haase, A. Trommer, P. Grundler, *Electroanalysis* **1994**, 6, 769–772.
- [5] W. J. Albery, W. N. Brooks, S. P. Gibson, M. W. Heslop, C. E. W. Hahn, *Electrochim. Acta* **1979**, 24, 107–108.
- [6] A. E. G. Cass, G. Davis, G. D. Francis, H. A. O. Hill, W. J. Aston, I. J. Higgins, E. V. Plotkin, L. D. L. Scott, A. P. F. Turner, *Anal. Chem.* **1984**, 56, 667–671.
- [7] S. Kuss, R. A. S. Couto, R. M. Evans, H. Lavender, C. C. Tang, R. G. Compton, *Anal. Chem.* **2019**, 91, 4317–4322.
- [8] a) K. Chaisiwamongkhol, C. Batchelor-McAuley, R. G. Compton, *Analyst* **2019**, 144, 1386–1393; b) ANB Sensors, can be found under <http://www.anbsensors.com>, 2020.
- [9] a) Zimmer Peacock, can be found under <https://www.zimmerpeacock.com>, 2020; b) Sensirion, can be found under <https://www.sensirion.com/en>, 2020; c) Metrohm DropSens, can be found under <http://www.dropsens.com>, 2020.
- [10] a) J. Wang, M. Jiang, F. Lu, *J. Electroanal. Chem.* **1998**, 444, 127–132; b) M. Gattrell, D. W. Kirk, *J. Electrochem. Soc.* **1993**, 140, 1534–1540; c) J. Iniesta, P. A. Michaud, M. Panizza, G. Cerisola, A. Aldaz, C. Comninellis, *Electrochim. Acta* **2001**, 46, 3573–3578; d) N. B. Tahar, A. Savall, *Electrochim. Acta* **2009**, 55, 465–469; e) J. M. Skowronski, P. Krawczyk, *J. Solid State Electrochem.* **2004**, 8, 442–447.
- [11] a) K. Chen, Z. L. Zhang, Y. M. Liang, W. Liu, *Sensors* **2013**, 13, 6204–6216; b) M. Del Pilar Taboada Sotomayor, A. A. Tanaka, L. T. Kubota, *J. Electroanal. Chem.* **2002**, 536, 71–81; c) B. Rezaei, M. K. Boroujeni, A. A. Ensaifi, *Electrochim. Acta* **2014**, 123, 332–339; d) R. Sha, S. K. Puttapati, V. V. S. S. Srikanth, S. Badhulika, *J. Electroanal. Chem.* **2017**, 785, 26–32; e) L. Fernández, C. Borrás, H. Carrero, *Electrochim. Acta* **2006**, 52, 872–884.
- [12] D. Hawley, R. N. Adams, *J. Electroanal. Chem.* **1965**, 10, 376–386.
- [13] a) Y. Uchida, E. Katelhon, R. G. Compton, *J. Electroanal. Chem.* **2018**, 818, 140–148; b) Y. Uchida, E. Katelhon, R. G. Compton, *J. Electroanal. Chem.* **2019**, 835, 60–66; c) Y. Wang, L. Chen, K. Chaisiwamongkhol, R. G. Compton, *Food Chem.* **2019**, 309, 125606.
- [14] C. Batchelor-McAuley, J. Ellison, K. Tschulik, P. L. Hurst, R. Boldt, R. G. Compton, *Analyst* **2015**, 140, 5048–5054.
- [15] R. Guidelli, R. G. Compton, J. M. Feliu, E. Gileadi, J. Lipkowski, W. Schmickler, S. Trasatti, *Pure Appl. Chem.* **2014**, 86, 245–258.
- [16] R. Niesner, A. Heintz, *J. Chem. Eng. Data* **2000**, 45, 1121–1124.
- [17] F. Bruno, M. C. Pham, J. E. Dubois, *Electrochim. Acta* **1977**, 22, 451–457.
- [18] M. D. Liptak, K. C. Gross, P. G. Seybold, S. Feldgus, G. C. Shields, *J. Am. Chem. Soc.* **2002**, 124, 6421–6427.
- [19] a) H. Bramwell, A. E. G. Cass, P. N. B. Gibbs, M. J. Green, *Analyst* **1990**, 115, 185–188; b) E. R. Lowe, C. E. Banks, R. G. Compton, *Anal. Bioanal. Chem.* **2005**, 383, 523–531; c) H. J. Salavagione, J. Arias, P. Garces, E. Morallon, C. Barbero, J. L. Vazquez, *J. Electroanal. Chem.* **2004**, 565, 375–383; d) C. Hoffman, M. de la Rosa, M. R. Anderson, C. Rhodine, W. G. Kuhr, *ECS Trans.* **2017**, 80, 1319–1332.
- [20] R. N. Adams, *Electrochemistry at solid electrodes*, Dekker, New York, 1969.
- [21] a) H. D. Gibbs, *J. Biol. Chem.* **1927**, 72, 649–664; b) J. R. Baylis, *J. Am. Water Works Assoc.* **1928**, 19, 597–604; c) J. C. Dacre, *Anal. Chem.* **1971**, 43, 589–591; d) M. B. Ettinger, C. C. Ruchhoft, *Anal. Chem.* **1948**, 20, 1191–1196.
- [22] a) Y. Uchida, E. Katelhon, R. G. Compton, *J. Electroanal. Chem.* **2018**, 823, 465–473; b) H. M. A. Amin, Y. Uchida, E. Katelhon, R. G. Compton, *J. Electroanal. Chem.* **2019**, 836, 62–67.

Manuscript received: July 13, 2020

Revised manuscript received: July 31, 2020

Accepted manuscript online: August 3, 2020